Radiotherapy and Oncology 179 (2023) 109456

Contents lists available at ScienceDirect

Radiotherapy and Oncology

journal homepage: www.thegreenjournal.com

Original Article

Dosimetric feasibility of direct post-operative MR-Linac-based stereotactic radiosurgery for resection cavities of brain metastases

Enrica Seravalli [a,*], Michelle Sierts [a], Eric Brand [a], Matteo Maspero [a], Szabolcs David [a], Mariellen E.P. Philippens [a], Eduward H.J. Voormolen [b], Joost J.C. Verhoeff [a]

[a] Department of Radiation Oncology; and [b] Department of Neuro Surgery, University Medical Centre Utrecht, the Netherlands

ARTICLE INFO

Article history:
Received 26 October 2022
Received in revised form 20 December 2022
Accepted 22 December 2022
Available online 30 December 2022

Keywords:
Brain metastasis
SRS
MRgART
Post-operative MRI

ABSTRACT

Background: Post-operative radiosurgery (SRS) of brain metastases patients is typically planned on a post-recovery MRI, 2–4 weeks after resection. However, the intracranial metastasis may (re-)grow in this period. Planning SRS directly on the post-operative MRI enables shortening this time interval, anticipating the start of adjuvant systemic therapy, and so decreasing the chance of extracranial progression. The MRI-Linac (MRL) allows the simultaneous execution of the post-operative MRI and SRS treatment. The aim of this work was investigating the dosimetric feasibility of MRL-based post-operative SRS.

Methods: MRL treatments based on the direct post-operative MRI were simulated, including thirteen patients with resectable single brain metastases. The gross tumor volume (GTV) was contoured on the direct post-operative scans and compared to the post-recovery MRI GTV.

Three plans for each patient were created: a non-coplanar VMAT CT-Linac plan (ncVMAT) and a coplanar IMRT MRL plan (cIMRT) on the direct post-operative MRI, and a ncVMAT plan on the post-recovery MRI as the current clinical standard.

Results: Between the direct post-operative and post-recovery MRI, 15.5 % of the cavities shrunk by > 2 cc, and 46 % expanded by $\geq$ 2 cc. Although the direct post-operative cIMRT plans had a higher median gradient index (3.6 vs 2.7) and median V3Gy of the skin (18.4 vs 1.1 cc) compared to ncVMAT plans, they were clinically acceptable.

Conclusion: Direct post-operative MRL-based SRS for resection cavities of brain metastases is dosimetrically acceptable, with the advantages of increased patient comfort and logistics.

Clinical benefit of this workflow should be investigated given the dosimetric plausibility.

Surgical resection of brain metastases is the standard of care for patients with good performance status and a single metastasis or with large metastases (>3cm) causing neurologic dysfunction or refractory edema. Post-operative stereotactic radiosurgery (SRS) aims to treat the surgical cavity to minimize the local relapse risk, even after complete resection [1]. SRS is typically delivered 2–4 weeks after surgery, but the optimal timing for post-operative therapy remains unclear [2].

Delaying SRS allows more time for logistical radiotherapy planning, patient recovery, wound healing and ultimately for resection cavity stabilization, thereby possibly decreasing the treatment volumes, which may, in turn, spare normal brain tissue and so reduce the risk of symptomatic radiation necrosis [3,4]. However, the concern with delaying cavity SRS is that the tumor may (re-)grow negatively impacting local and systemic control [5].

The timing of SRS relative to checkpoint inhibitor-based immunotherapy (IT) is critical to best exploit their synergistic effects. El Jalby found that timing depends on the immunotherapeutic agent choice and as long as IT follows SRS with a start within four weeks, consistent benefits are realized in the outcomes compared with SRS or IT alone [6].

The current brain metastases workflow at our academic hospital leads to an average IT treatment-free interval of six weeks, consisting of surgery followed by SRS after recovery. However, shortening this interval to less than a week improves the overall survival in melanoma patients with brain metastases [7].

Another factor influencing IT treatment effectiveness is supplementation of dexamethasone, given pre-operatively and again as a precaution around SRS [8]. Shortening the interval between the two modalities leads to a single tapering period and thus a faster IT start.

Simply starting IT prior to post-operative SRS is not a safe solution, as dexamethasone reduces its effectiveness [9].

* Corresponding author at: Department of Radiation Oncology, University Medical Centre Utrecht, Postbox 85500, 3508 GA Utrecht, the Netherlands.
E-mail address: e.seravalli@umcutrecht.nl (E. Seravalli).

https://doi.org/10.1016/j.radonc.2022.109456
0167-8140/

This work explores the application of MRI-guided radiotherapy (MRgRT) technology to enable SRS during post-operative magnetic resonance imaging (MRI).

MRgRT combines magnetic resonance imaging with a radiation therapy system, allowing real-time MR imaging, improved soft-tissue contrast of target volumes and organs at risk (OAR) before, during, and after treatment delivery, and online adaptive re-planning [10].

Slagowski evaluated the dosimetric feasibility of single target brain SRS with the MRIdian system [11]. He concluded that the MR-Linac (MRL) system could produce clinically acceptable SRS plans for spherical lesions with a diameter $\leq$ 2.25 cm. Wen showed that the required plan quality and accuracy for treating brain metastasis with a single isocenter on the MRL could be achieved [12].

Using the MRgRT workflow to treat resection cavities allows radiation delivery directly during the post-operative MRI, which minimizes the interval between the treatments (Fig. 1), allows an earlier IT start and reduces the chance of tumor shifts due to dexamethasone use [13].

Moreover, logistics and patient comfort could be improved because the post-recovery MRI becomes obsolete and the patient does not need to return to the hospital after 2–4 weeks for the radiotherapy preparation.

The feasibility of an MRgRT workflow for resection cavities directly based on the post-operative MRI has not yet been reported in the literature. The main concerns are the higher dose that the healthy brain could be exposed to due to (1) a presumably larger cavity volume to irradiate immediately after surgery compared to 2–4 weeks later and (2) different MRL technical aspects affecting the dose gradient, e.g. only coplanar beams, wider multi-leaf-collimator (MLC) leaves at the isocenter [14,15].

This study investigates the dosimetric quality of single brain metastasis resection cavity MRL SRS treatment plans made directly on the post-operative MRI. In particular, the healthy brain dose between the direct post-operative and post-recovery MRI-based dose distribution is compared.

Methods and materials

This retrospective in-silico study was approved by the local ethics committee (approval letter number 17/906). Writing of the manuscript was steered by the RATING guidelines for reporting treatment planning studies [16].

Patient cohort

Thirteen consecutive patients with resected single brain metastasis treated at the University Medical Center Utrecht between January and June 2017 with cone-beam computed tomography linac (CT-Linac) non-coplanar VMAT-based stereotactic radiotherapy were selected for the analysis in this study. All patients were treated in a single fraction prescribed at 100 % isodose varying from 15 Gy up to 21 Gy depending on the cavity size according to the Dutch consensus protocol for brain metastasis radiotherapy (Table 1).

Imaging and delineation

For the included patients, a median interval of 29 days between resection and SRS was registered. Directly pre-operative and post-operative MRIs were acquired 1 day before and 2 days (median) after surgery. The post-recovery MRI during radiotherapy preparation was performed 20 days (median) after surgery. A 1.5 T MRI

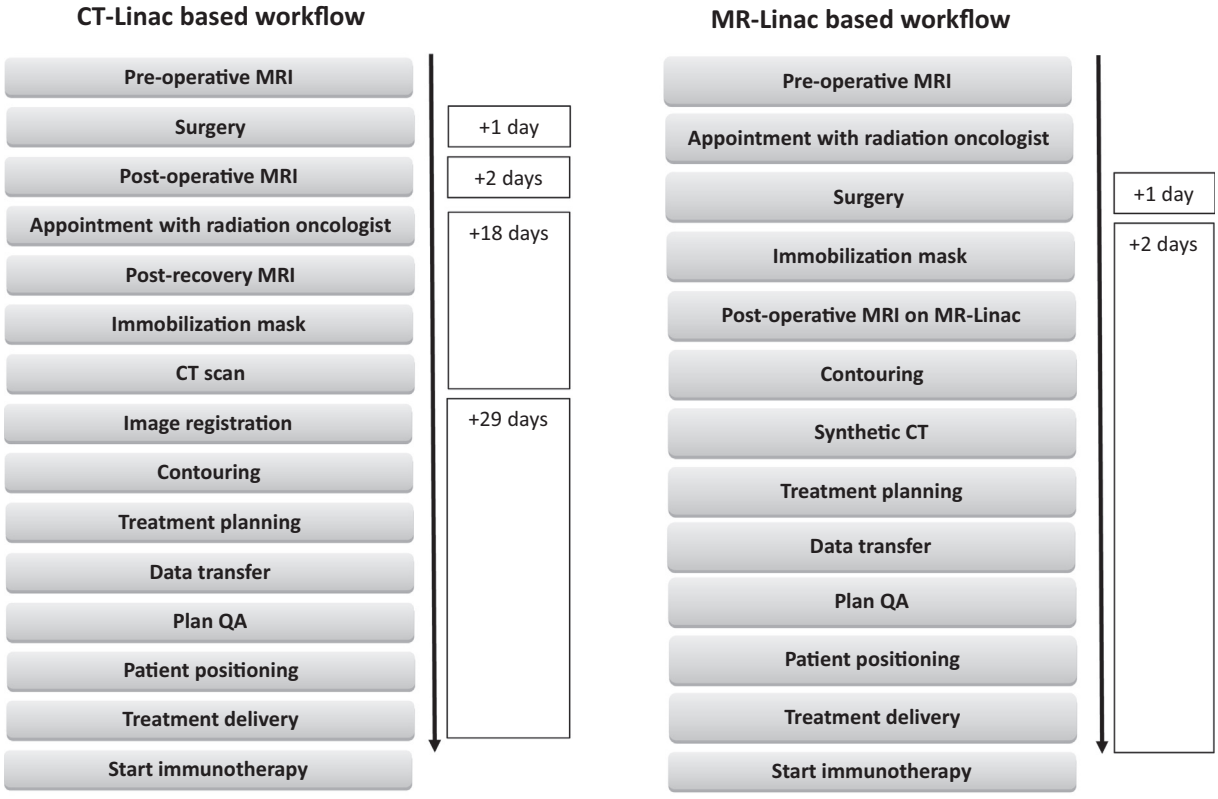

Fig. 1. Treatment workflow for resection cavities of brain metastasis on a CT-Linac and MR-Linac with corresponding timeline that starts with the pre-operative MRI (day 0). In the MR-Linac based workflow the post-operative MRI is performed directly on this system while the post-recovery MRI together with the CT scan are omitted.

Table 1
Patient characteristics, describing age, sex, metastasis location, primary tumor, the GTV (in cc) on pre-operative, post-operative, and post-recovery MRI, and the time interval between post-operative and post-recovery MRI (in days).

Patient	Age	Sex	Metastasis location	Primary tumor	GTV (cc)			Change in GTV (%) between post-op and post-rec	Prescribed dose (Gy)		Time interval between post-op and post-rec MRI (d)
					Pre-op MRI	Post-op MRI	Post-rec MRI		Post-op plan	Post-rec plan	
1	64	F	Right frontal	NSCLC (adeno)	3.7	1.3	5.1	75	21.0	21.0	21
2	56	F	Right cerebellum	NSCLC (adeno)	7.3	5.6	5.4	−4	18.0	21.0	15
3	76	M	Right parietal	Colon CA (adeno)	8.4	7.1	9.2	23	18.0	18.0	16
4	79	F	Right parieto-occipital	NSCLC (adeno)	9.1	3.7	25.2	85	21.0	15.0	10
5	58	F	Right frontal	NSCLC (adeno)	14.1	11.8	17.2	31	15.0	15.0	28
6	70	F	Left parieto-occipital	NSCLC (adeno)	20.9	11.1	12.2	9	18.0	18.0	18
7	84	M	Right parieto-occipital	NSCLC (adeno)	21.9	10.8	9	−20	18.0	18.0	20
8	68	M	Right frontal	Melanoma	24.1	8.1	13.8	41	18.0	18.0	20
9	56	F	Right parieto-occipital	Breast CA (adeno)	40.4	32.2	42.7	25	15.0	15.0	13
10	52	F	Left frontal	Adeno CA, unknown primary.	55.6	29.8	43.9	32	15.0	15.0	12
11	50	F	Right temporo-occipital	NSCLC (adeno)	62	16.5	9.9	−67	15.0	18.0	15
12	52	M	Left fronto-parietal	NSCLC (adeno)	64.1	13.7	15.4	11	15.0	15.0	21
13	61	M	Left parietal	NSCLC (adeno)	82.6	27.4	8.7	−215	15.0	18.0	16
Median	63.5				21.9	11.1	12.2				16
Range	50–84				3.7–82.6	1.3–29.8	5.1–43.9				10–28

(Ingenia; Philips Medical System, The Netherlands) protocol was acquired containing a 3D T1 spoiled gradient echo (T1-TFE) gadolinium-enhanced scan with a 1x1x1 mm^3 reconstructed resolution [17].

The radiotherapy preparation also included a planning CT scan (Brilliance, Philips Medical Systems, The Netherlands) with a 1 mm slice thickness carried out in a frameless head immobilization device (Civco Medical Solutions, Kalona, Iowa, USA) combined with individual head support [18].

For each patient all images were transferred to the delineation software, and the post-recovery MRI sequences were registered to the planning CT by rigid mutual information on a box around the skull at the level of the tumor [19].

On the T1-weighted post gadolinium injection sequence, a radiation oncologist manually defined the gross tumor volume (GTV) on the three different MRI time points as the residual T1-weighted gadolinium-enhancing area plus resection cavity. Contoured organs at risk (OAR) included the eyeballs, lenses, optic nerves, optic chiasm, brainstem, cochlea, pituitary gland, total brain, according to Tseng [20], and skin (defined as a 3 mm rim of tissue up to the tissue-air boundary at the patient surface).

The wound complications occurrence is one of the concerns when radiotherapy and surgery are combined in a short time frame. Therefore, the surgery wound on the scalp of the patient was delineated to assess the dose received by this volume.

For MRL treatment planning purposes, a synthetic CT (sCT) was generated from the directly post-operative T1 3D sequence according to a previously published method [21].

Afterwards, the post-operative sCT and the post-recovery CT were imported into the treatment planning system. For VMAT plans on an Elekta CT-Linac, a 1 mm planning target volume (PTV) was generated via a geometric circumferential expansion beyond the GTV, and a 2 mm PTV for Unity MRL plans.

Treatment planning

Two treatment planning techniques were considered:

- a non-coplanar VMAT (ncVMAT) technique for treatment on an Elekta CT-linac equipped with Agility head (consisting of 80 MLC leaf pairs with a leaf width of 5 mm at isocenter): 6 MV 2 non-coplanar arcs, one full and one partial (gantry 30-180°) at 0°- and 90°-couch angle according to the institutional protocol.

- a coplanar IMRT (cIMRT) technique for treatment on an Unity MRL system (80 MLC leaf pairs with a leaf width of 7.2 mm at isocenter): 7 MV coplanar non-opposing 13-beams technique.

Treatment planning was performed in a Monaco (TPS) (Elekta AB, Stockholm, Sweden), version 5.11.02 for VMAT plans, and version 5.51.10 for IMRT plans using a Monte Carlo dose calculation algorithm. All plans were created to achieve at least 98 % PTV coverage with 100 % of the prescription dose. A point maximum of less than 130 % of the prescription dose was allowed within the PTV. OAR constraints and optimization prioritizing are shown in Appendix 1. The dose grid size was $2 \times 2 \times 2$ mm^3 according to the institutional protocol (compromise between computation time and dose calculation accuracy). A 3 % statistical uncertainty per control point was used for ncVMAT plans (to ensure that the total uncertainty at the dose reference point is less than 0.5 %), a maximum of 144 control points per arc and a minimum segment width of 0.5 cm was allowed as per institutional protocol. The cIMRT plans were computed with a statistical uncertainty of 3 % per control point, a minimum of 5.0 MU per segment, and a minimum width of 0.5 cm.

Three single fraction plans per patient were created: ncVMAT and cIMRT for the GTV defined on the directly post-operative MRI and ncVMAT for the GTV defined on the post-recovery MRI. The ncVMAT dose distribution delivered by a CT-Linac was considered the "reference standard" in this study as this is the current clinical practice at our institute. Therefore, ncVMAT plans were also created for the post-operative GTV to allow a direct comparison to the cIMRT dose distribution independently of target volume differences.

Plans, generated by the same experienced planner, were made such that the PTV coverage was comparable in the three situations allowing iterative modifications to the objective functions after each dose calculation to yield the best possible plan.

Plan evaluation and comparison

The resection cavity (GTV) volume defined on the three MRI's was computed and compared among the acquisition time points.

Clinically relevant dosimetric parameters in the context of brain SRS were chosen a priori to enable dose distribution comparison consisting of V100% (volume of PTV receiving at least 100 % of the prescription dose); the V2Gy, V5Gy, V12Gy and V14Gy (vol-

umes receiving at least 2 Gy, 5 Gy, 12 Gy and 14 Gy, respectively) and the mean dose of (Brain – GTV). Moreover, the volume of skin receiving at least 3 Gy was calculated together with the mean dose and the dose received by 0.1 cc of the skin and the surgery wound mean dose.

Conformity was assessed using the Paddick Conformity Index (CI) [22]:

$$CI = \frac{(TV_{PIV})^2}{(TV \times PIV)}$$

where TV_{PIV} is the target volume covered by the prescription isodose, TV is the target volume, and PIV is the prescription isodose volume. The value of CI ranges from 0.0 to 1.0, with 1.0 representing perfect conformity. The Paddick Gradient Index (GI) was also calculated to objectively measure dose fall-off outside the target [23]:

$$GI = \frac{PIV_{HALF}}{PIV}$$

where PIV_{HALF} is the volume covered by half of the prescription dose and PIV is the prescription isodose volume. A low GI indicates a low dose spread outside the lesion and a sharp dose fall-off.

Statistical analysis

Descriptive statistics (median, mean and standard deviation) were used to summarize dosimetric parameters. The differences between selected dosimetric parameters were assessed by the Wilcoxon signed-rank test using paired comparison. All statistical tests were two-sided, and statistical significance was defined at the $p < 0.05$ threshold. Statistical analyses were performed using SPSS version 25 (IBM corporation).

Results

From pre-operative to direct post-operative MRI, 9/13 (69 %) lesions shrunk while 4/13 (31 %) lesions remained stable in size (defined as a change in volume of $\leq$ 2 cc) (Fig. 2). Between the direct post-operative and post-recovery MRI, 2/13 (15.5 %) cavities shrunk by > 2 cc, 5/13 (38.5 %) cavities remained stable in size (<2 cc volume change) and the majority 6/13 (46 %) expanded by > 2 cc.

Due to GTV volume changes from the post-op to the post-recovery situation the prescribed dose for 4 patients changed between the two time points (Table 1): for patient 2, 11 and 13 the prescribed dose increased while for patient 4 decreased in the post-recovery situation.

Target coverage (Table 2) and OAR constraints (data not shown) were met for all types of plans and patients. An example of post-operative ncVMAT and cIMRT dose distribution, in 3 orthogonal views, is depicted in Fig. 3. The median CI (0.9) is the same for the three considered situations. Compared to the cIMRT plans, the median GI is smaller for ncVMAT plans (post-op: 2.7 vs 3.6). The volume of the (Brain – GTV) receiving 2 Gy (p =.003), 5 Gy (p =.001), 12 Gy (p =.001), and 14 Gy (p =.001) of cIMRT plans is significantly higher compared to post-op ncVMAT plans (Fig. 4). The V2Gy (p =.507), V5Gy (p =.600), V12Gy (p =.463) and V14Gy (p =.969) of post-op ncVMAT plans are comparable to the one based on the post-recovery MRI. An increase in V3Gy of skin (in cc) is observed for cIMRT plans for all patients compared to post-op ncVMAT plans (p =.001) (Fig. 5). The median skin V3Gy of post-op cIMRT plans is 17,3 cc larger than the one for post-op ncVMAT plans. The median surgery wound mean dose is 2.5 Gy (range: 1.4–3.8 Gy) for the cIMRT plans and 1.4 Gy (range: 0.8–2.2 Gy) for post-op ncVMAT plans (p =.001).

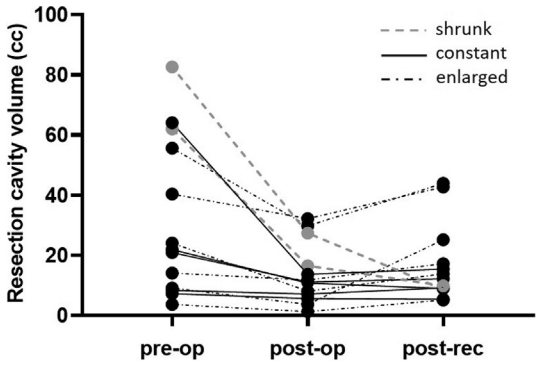

Fig. 2. Volume of the resection cavity (cc) defined on the pre-operative, post-operative, and post-recovery MRI. A dashed grey line indicates cavities that shrunk between the post-operative and post-recovery MRI, a solid black line indicates cavities that remain stable in size and a dashed-dot black line indicates cavities that enlarged.

Discussion

Treatment plans for post-operative and post-recovery time points and coplanar IMRT and no-coplainr VMAT were analysed to assess the dosimetric feasibility of brain metastases resection cavities SRS during direct post-operative MRI acquisition on the MR-Linac.

MRL SRS planning using the direct post-operative MRI is feasible as all clinical planning objectives for target coverage and OAR were met.

Cavity volume changes between the post-operative and post-recovery MRI were observed in 8/13 patients. Cavity volume variations can be caused by steroids and chemotherapy [13]. Patel showed that resection cavities increased in volume from the post-operative to the post-recovery MRI [24]. When considering SRS immediately after surgery, only in 2/13 cases of the study cohort, larger cavities would be irradiated compared to the post-recovery volume. For these two cases (patients 11 and 13), the mean healthy brain dose in the direct post-operative situation is 1 Gy higher than the post-recovery ncVMAT dose, while the V12Gy increases by 8 cc and 29 cc, respectively. According to Fig. 3a of Milano [25], this increase corresponds to about 9 % (0.39 vs 0.48 for patient 11) and 15 % (0.35 vs 0.50 for patient 13) higher probability of developing any radionecrosis. These two cases would profit from a longer interval between surgery and SRS in terms of radionecrosis probability after irradiation.

Atalar did not find significant cavity volume changes between the immediate post-operative and the post-recovery MRI up to 33 days after surgery for most patients [26]. In contrast, another study reported that 46.5 % cavities were stable in size, defined as a change in volume of < 2 cc, but 23.3 % shrunk by > 2 cc, and about the same proportion enlarged by > 2 cc [5].

In this study, the majority (69 %) of the lesions delineated on the pre-operative MRI shrunk > 2 cc when considering the post-operative MRI. According to the Dutch national protocol, that is partly based on the results of Minnitti [27], the prescribed dose depends on the (cavity) volume. Therefore, due to the observed volume variation the prescribed dose of the plan based on the pre-operative scan, used as a pre-treatment plan for the MR-Linac workflow, needs to be modified when starting the online adaptive workflow based on the post-operative scan, requiring extra treatment planning time (on average 6 min, data not shown).

The gradient index and healthy brain dose favor ncVMAT plans. The differences observed between post-op cIMRT and ncVMAT plans are explained by the different technical delivery aspects of MRL and CT-Linac, such as coplanar versus non-coplanar beam

Table 2
Dosimetric endpoints for the 13 patients for post-operative (post-op) and post-recovery (post-rec) ncVMAT and post-operative cIMRT dose distributions. GI = gradient index, CI = conformity index, V100%=volume receiving at least 100 % of the prescription dose, Dmean = mean dose, D0.1 cc = dose received by 0.1 cc.

Patient	PTV						Brain-GTV			Skin					
	V100%			GI		CI				Dmean (Gy)			D0.1 cc(Gy)		
	post-op	post-op	post-rec	post-op	post-op	post-rec	post-op	post-op	post-rec	post-op	post-op	post-rec	post-op	post-op	post-rec
	cIMRT	ncVMAT	ncVMAT	cIMRT	ncVMAT	ncVMAT	cIMRT	ncVMAT	ncVMAT	cIMRT	ncVMAT	ncVMAT	cIMRT	ncVMAT	ncVMAT
1	97.9	97.7	97.3	4.4	3.6	3.4	0.8	0.8	0.8	0.8	0.6	1.0	0.4	0.6	0.3	7.4	4.9	12.1
2	98.2	98.0	98.6	3.9	3.0	2.9	0.8	0.8	0.9	1.7	1.5	1.4	0.6	0.3	0.2	6.3	4	3.3
3	97.7	97.6	97.6	3.7	2.7	2.6	0.9	0.9	0.9	1.3	1.1	1.1	0.5	0.3	0.2	6.3	4.1	4.5
4	98.3	98.2	98.5	4.1	3.1	2.3	0.8	0.8	0.9	1.3	0.9	1.5	0.6	0.3	0.5	6.9	4.3	11.3
5	97.5	97.7	97.7	3.4	2.6	2.6	0.9	0.9	0.9	1.6	1.3	1.2	0.7	0.4	0.3	6.5	4.7	5.9
6	98.1	98.1	97.5	3.5	2.6	2.5	0.9	0.9	0.9	1.9	1.5	1.4	0.7	0.4	0.2	7.1	3.9	4
7	97.3	97.2	97.7	3.6	2.6	2.6	0.9	0.9	0.9	1.4	1.1	1.0	0.6	0.3	0.2	6.2	3.7	3.8
8	97.9	97.8	97.9	3.7	2.7	2.5	0.9	0.9	0.9	1.3	0.1	1.0	0.5	0.3	0.2	5.9	3.4	5.2
9	96.0	96.5	97.6	3.2	2.4	2.2	0.9	0.9	1.0	2.4	1.9	2.0	0.9	0.5	0.4	6.3	4.2	4.3
10	98.4	98.3	98.6	2.8	2.4	2.3	0.9	0.8	0.9	2.5	2	2.0	1.1	0.7	0.6	9.2	6.9	4.3
11	97.6	97.8	97.2	3.5	2.7	2.8	0.9	0.8	0.8	2.1	1.5	1.3	0.8	0.4	0.4	7.2	3.7	5.4
12	97.6	97.6	97.9	3.6	2.7	2.6	0.9	0.9	1.0	1.6	1.5	1.3	0.7	0.4	0.2	5.1	3	2.7
13	98.3	98.2	98.8	3.5	2.4	2.7	0.9	0.9	0.9	1.9	1.6	1.0	0.9	0.4	0.3	7.5	3.4	3.8
Median	97.9	97.8	97.7	3.6	2.7	2.6	0.9	0.9	0.9	1.6	1.5	1.3	0.7	0.4	0.3	6.5	4.0	4.3
Average	97.8	97.7	97.9	3.6	2.7	2.6	0.9	0.9	0.9	1.7	1.3	1.3	0.7	0.4	0.3	6.8	4.2	5.4
Std	0.6	0.5	0.5	0.4	0.3	0.3	0.0	0.0	0.0	0.5	0.5	0.3	0.2	0.1	0.1	1.0	1.0	2.9
p	0.410	0.325		0.001	0.077		0.180	0.25		0.004	0.893		0.001	0.018		0.116	0.100	

arrangement, projected MLC leaf width at the isocenter, and PTV margin. While the differences between post-op and post-recovery ncVMAT plans are caused by cavity volume changes.

The higher dose to the healthy brain tissue in cIMRT plans is in agreement with literature, although clinical relevance is not clear [11,28]. The dosimetric benefit of a smaller projected MLC leaf width of non-coplanar techniques has been demonstrated before [29 30 31–36].

The technical differences between MR-Linac and CT-Linac give rise to specific patient selection for each workflow. For patients with multiple brain metastases or for certain locations, e.g. close to an organ at risk or in between the eyes, a non-coplanar CT-Linac irradiation technique would be preferable due to the steeper dose fall. Due to the dosimetric advantage of smaller projected MLC leaf width at the isocenter, very small lesions (<2 cc) would be better treated on a CT-Linac. Patients with expected target volume changes would benefit of MRI guidance (in particular of an Adapt-to-Shape workflow), especially during fractioned SRS [37,38].

The skin volume receiving a higher dose was found to be larger for MRL plans. This is mainly due to the Electron Return Effect: secondary electrons exiting tissue into the air being curved back to deposit dose at the tissue surface due to the Lorentz force, which results from the presence of the magnetic field perpendicular to the beam direction [39,40]. Wang also found skin doses significantly higher for MRL plans and correlated this with in vivo measurements for glioma patients [41]. A potential strategy to mitigate skin dose during MR-Linac treatment could be using a skin objective during planning optimization. Wang demonstrated that Monaco's Monte Carlo dose algorithm could accurately model the near-surface dose, and using the TPS IMRT optimizer with skin as an avoidance structure can reliably decrease skin dose [41]. While the importance of alopecia in affecting the long-term quality of life has been recognized, it has been accepted as an unavoidable consequence after brain radiotherapy [42]. Recent normal tissue complication probability models for temporal alopecia suggest that the alopecia probability is dose-dependent with no apparent threshold [43].

The occurrence of wound complications is one of the concerns when radiotherapy and surgery are combined in a short time frame, regardless of the order of execution. For keloid brachytherapy no severe wound healing effects are described [44]. Wound complication rates of up to 46 % have been reported when radiotherapy and surgery were combined less than a week apart [45]. Besides the time interval between surgery and radiotherapy other factors including incision size, radiation dose, number of fractions and patient related factors are important for the wound complications risk [46]. Kumar investigated the effect of different radiation doses on wound healing in albino mice: a wound dose of 2 Gy already resulted in delayed healing compared with a wound without radiation exposure [47]. For both post-operative considered plan types the median wound mean dose was $\leq$ 2 Gy.

Consensus cavity contouring guideline would suggest inclusion of a dural margin of 5–10 mm [48]. This could potentially further increase complication rates given the proximity of the dura to the wound. Not all resected metastases have a dural component, therefore patient selection prior to inclusion in the directly postoperative SRS workflow should be performed by specialists.

The theoretical dosimetric disadvantages of post-op cIMRT plans must be weighed against the benefits of the immediate post-operative radiotherapy treatment: faster treatment trajectory for the patient, enabling a month earlier start of adjuvant systemic therapies for better extracranial disease control, and improved logistics. Since patients with metastatic disease are frequently older, such initiatives are precious for quality of life. Furthermore, the SRS treatment is administered while the patient is under

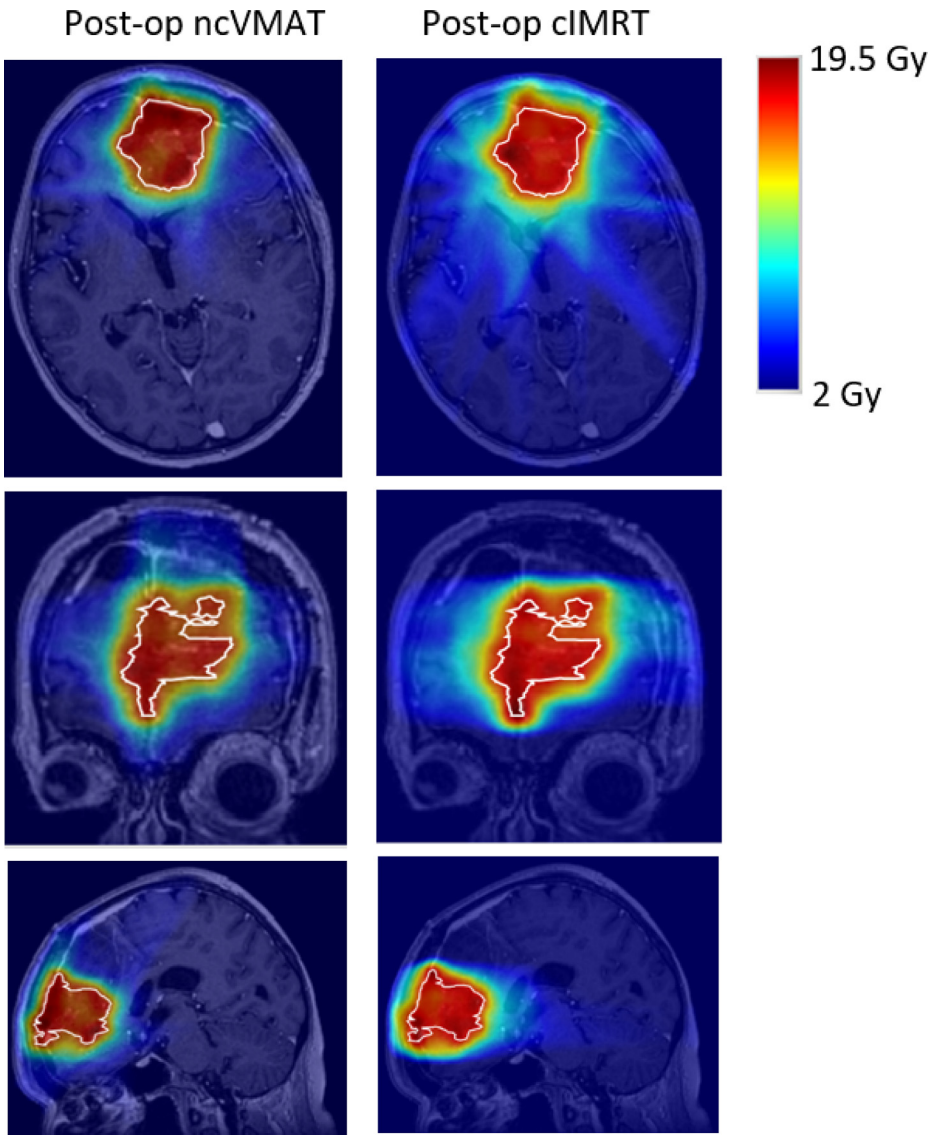

Fig. 3. Dosimetric distribution, in 3 orthogonal views, for patient #11 with a prescription dose of 15 Gy single fraction. The ncVMAT plan is shown on the left and the cIMRT plan on the right. The post-operative GTV corresponds to the white line.

supervision of the clinical neurosurgery ward and receives clinical dexamethasone tampering regimens and not as a less supervised out-patient. The alternative to fast sequential treatment - administering SRS during targeted therapies, may lead to a 2.4 higher risk for symptomatic radionecrosis and is, therefore, less attractive [49].

To shorten the standard treatment workflow for brain metastases resection cavities while maintaining the ncVMAT dosimetric distribution, a direct post-operative CT-Linac workflow could be adopted. In this case imaging and treatment delivery would occur on two different systems and the overall time would increase by at least one day compared to the MRL workflow. Moreover, this would mean less comfort for the patient with two separate sessions instead of one.

Besides the dosimetry, the feasibility of an MRgRT workflow for resection cavities based on direct post-operative MRI also depends on solving other issues such as image quality of the MRI acquired on the MRL compared to a diagnostic MRI, injection of Gadolinium contrast agent shortly (about 15–30 min) before radiation delivery, and personalizing an immobilization head mask with the fresh surgery scar still in place. Moreover, a model predicting cavity changes would be needed to select patients that could profit of the direct post-op SRS MR-Linac workflow instead of the standard of care workflow. However, these issues fall outside of the scope of the current study.

New strategies to enhance local control and minimize the risk of leptomeningeal disease include pre-operative SRS [50]. An SRS MRL workflow could also be used for this type of treatment choice.

This study is limited by its in-silico retrospective nature, with all patients treated at a single center. The interval between resection and post-operative SRS was neither uniform nor predefined in the considered cohort. This was mostly due to: availability of MRI capacity, patient condition, or adjustment of timing of systemic therapy. Another possible limitation is the limited size of the cohort generating only 39 plans. Moreover, the reproducibility of study observations could be a limitation since treatment plans are operator dependent and were all made by an experienced radiation technologist.

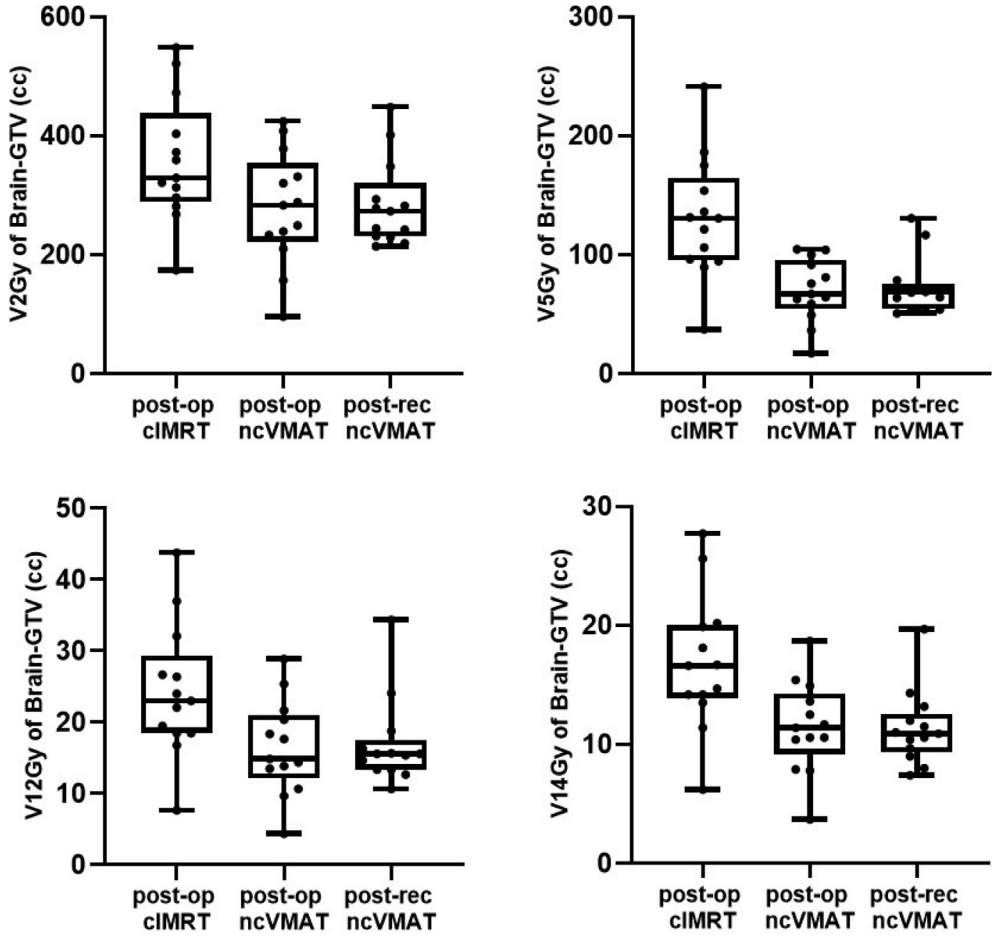

Fig. 4. Boxplot of dosimetric endpoints reporting the volume of (Brain – GTV) receiving 2 Gy, V5Gy, V12Gy, and V14Gy for post-operative cIMRT and ncVMAT and post-recovery ncVMAT plans.

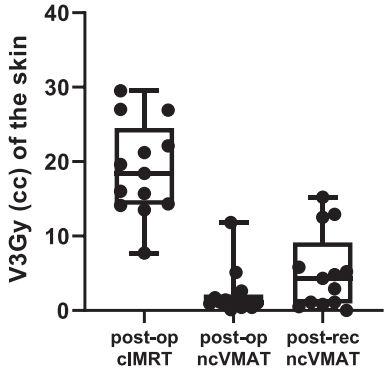

Fig. 5. Boxplot of V3Gy of the skin (in cc) for post-operative cIMRT and ncVMAT and post-recovery ncVMAT plans.

Conclusion

MR-Linac based SRS planning to brain metastases resection cavities using the direct post-operative MRI is feasible. The less favorable dose fall-off of MR-Linac plans, compared to non-coplanar VMAT CT-Linac plans, should be weighed against the faster trajectory for the patient, enabling an earlier start of adjuvant systemic therapies. The clinical acceptability of the investigated workflow depends on demonstration of safety compared to the standard workflow, 2–4 weeks after surgery.

Declaration of Competing Interest

The authors declare that they have no known competing financial interests or personal relationships that could have appeared to influence the work reported in this paper.

Appendix A. Supplementary material

Supplementary data to this article can be found online at https://doi.org/10.1016/j.radonc.2022.109456.

References

[1] Mahajan A et al. Post-operative stereotactic radiosurgery versus observation for completely resected brain metastases: a single-centre, randomised, controlled, phase 3 trial. Lancet Oncol 2017;18:1040–8.
[2] Ahmed S. Postoperative stereotactic radiosurgery for resected brain metastasis. CNS Oncol 2014;3:199–207.
[3] Shah JK et al. Surgical cavity constriction and local progression between resection and adjuvant radiosurgery for brain metastases. Cureus 2016;8:e575.
[4] Alghamdi M. Stereotactic radiosurgery for resected brain metastasis: cavity dynamics and factors affecting its evolution. J Radiosurg SBRT 2018;5:191–200.
[5] Jarvis LA et al. Tumor bed dynamics after surgical resection of brain metastases: implications for postoperative radiosurgery. Int J Radiat Oncol Biol Phys 2012;84:943–8.
[6] ElJalby M et al. Optimal timing and sequence of immunotherapy when combined with stereotactic radiosurgery in the treatment of brain metastases. World Neurosurg 2019;127:397–404.
[7] Wegner RE et al. Time from stereotactic radiosurgery to immunotherapy in patients with melanoma brain metastases and impact on outcome. J Neurooncol 2021;152:79–87.

[8] Jessurun CAC et al. The combined use of steroids and immune checkpoint inhibitors in brain metastasis patients: a systematic review and meta-analysis. Neuro Oncol 2021;23:1261–72.
[9] Martin AM et al. Immunotherapy and symptomatic radiation necrosis in patients with brain metastases treated with stereotactic radiation. JAMA Oncol 2018;4:1123–4.
[10] Cao Y et al. MR-guided radiation therapy: transformative technology and its role in the central nervous system. Neuro Oncol 2017;19. p. ii16-ii29.
[11] Slagowski, *Dosimetric feasibility of brain stereotactic radiosurgery with a 0 35 T MRI-guided.* Medical Physics, 2020. **47**: p. 5455-5466
[12] Wen N et al. Evaluation of a magnetic resonance guided linear accelerator for stereotactic radiosurgery treatment. Radiother Oncol 2018;127:460–6.
[13] Hessen ED et al. Significant tumor shift in patients treated with stereotactic radiosurgery for brain metastasis. Clin Transl Radiat Oncol 2017;2:23–8.
[14] Kluter S. *Technical design and concept of a 0.35 T MR-Linac.* Clin Transl. Radiat Oncol 2019;18:98–101.
[15] Raaymakers BW et al. First patients treated with a 1.5 T MRI-Linac: clinical proof of concept of a high-precision, high-field MRI guided radiotherapy treatment. Phys Med Biol 2017;62:L41–50.
[16] Hansen CR et al. Radiotherapy Treatment plannINg study Guidelines (RATING): a framework for setting up and reporting on scientific treatment planning studies. Radiother Oncol 2020;153:67–78.
[17] Nagtegaal SHJ et al. Does an immobilization mask have added value during planning magnetic resonance imaging for stereotactic radiotherapy of brain tumours? Phys Imaging Radiat Oncol 2020;13:7–13.
[18] Houweling AC et al. Improved immobilization using an individual head support in head and neck cancer patients. Radiother Oncol 2010;96:100–3.
[19] Bol GH et al. Simultaneous multi-modality ROI delineation in clinical practice. Comput Methods Programs Biomed 2009;96:133–40.
[20] Tseng CL et al. Glioma consensus contouring recommendations from a MR-Linac International Consortium Research Group and evaluation of a CT-MRI and MRI-only workflow. J Neurooncol 2020;149:305–14.
[21] Dinkla AM et al. MR-only brain radiation therapy: dosimetric evaluation of synthetic CTs generated by a dilated convolutional neural network. Int J Radiat Oncol Biol Phys 2018;102:801–12.
[22] Paddick, A simple scoring ratio to index the conformity of radiosurgical treatment plans.pdf>. J Neurosurg 2000. **93**: p. 219-222
[23] Paddick, *A simple dose gradient measurement tool to complement the conformity index.pdf>*. Journal of Neurosurgery, 2006. **105**: p. 194-201
[24] Patel RA et al. Postsurgical cavity evolution after brain metastasis resection: how soon should postoperative radiosurgery follow? World Neurosurg 2018;110:e310–4.
[25] Milano MT et al. Single- and multifraction stereotactic radiosurgery dose/volume tolerances of the brain. Int J Radiat Oncol Biol Phys 2021;110:68–86.
[26] Atalar B et al. Cavity volume dynamics after resection of brain metastases and timing of postresection cavity stereotactic radiosurgery. Neurosurgery 2013;72:180–5. discussion 185.
[27] Minniti G, Clarke E, Lanzetta G, Osti MF, Trasimeni G, Bozzao A, et al. Stereotactic radiosurgery for brain metastases: analysis of outcome and risk of brain radionecrosis. Radiat Oncol 2011;6:48.
[28] Tseng CL et al. Dosimetric feasibility of the hybrid Magnetic Resonance Imaging (MRI)-linac System (MRL) for brain metastases: the impact of the magnetic field. Radiother Oncol 2017;125:273–9.
[29] Serna A et al. Influence of multi-leaf collimator leaf width in radiosurgery via volumetric modulated arc therapy and 3D dynamic conformal arc therapy. Phys Med 2015;31:293–6.
[30] Dhabaan, *Dosimetric performance of the new high-definition multileaf collimator for intracranial stereotactic radiosurgery.* JOURNAL OF APPLIED CLINICAL MEDICAL PHYSICS,, 2010. **11**: p. 197.
[31] Audet, Evaluation of volumetric modulated arc therapy for cranial radiosurgery using multiple.pdf>. Medical Physics, 2011. **38**: p. 5863-5872
[32] Thomas EM et al. Comparison of plan quality and delivery time between volumetric arc therapy (RapidArc) and Gamma Knife radiosurgery for multiple cranial metastases. Neurosurgery 2014;75:409–17. discussion 417–8.
[33] Alongi F et al. First experience and clinical results using a new non-coplanar mono-isocenter technique (HyperArc) for Linac-based VMAT radiosurgery in brain metastases. J Cancer Res Clin Oncol 2019;145:193–200.
[34] Raymond P. Coplanar versus noncoplanar intensity-modulated radiation therapy (IMRT) and volumetric-modulated arc therapy (VMAT) treatment planning for fronto-temporal high-grade glioma. J Appl Clin Med Phys 2012;5:3826.
[35] Clark GM et al. Plan quality and treatment planning technique for single isocenter cranial radiosurgery with volumetric modulated arc therapy. Pract Radiat Oncol 2012;2:306–13.
[36] Liu H et al. Plan quality and treatment efficiency for radiosurgery to multiple brain metastases: non-coplanar RapidArc vs. Gamma knife. Front Oncol 2016;6:26.
[37] Tan H et al. Inter-fraction dynamics during post-operative 5 fraction cavity hypofractionated stereotactic radiotherapy with a MR LINAC: a prospective serial imaging study. J Neurooncol 2022 Feb;156:569–77.
[38] Hessen E et al. Predicting and implications of target volume changes of brain metastses during fractionated stereotactic radiosurgery. Radiother Oncol 2020. Jan.;142:175–9.
[39] Chen H. Technical note dose effects of 1 5 T transverse magnetic field on tissue interfaces. Med Phys 2016;43:4797.
[40] Hackett SL et al. Spiraling contaminant electrons increase doses to surfaces outside the photon beam of an MRI-linac with a perpendicular magnetic field. Phys Med Biol 2018;63:095001.
[41] Wang MH et al. Clinically Delivered Treatment for Glioma Patients on a Hybrid Magnetic Resonance Imaging (MRI)-Linear Accelerator (MR-Linac). and a Cone Beam CT (CBCT)-Guided Linac: Dosimetric Comparisons with In Vivo Skin Dose Correlation. Research square; 2021.
[42] Palma G et al. Modelling the risk of radiation induced alopecia in brain tumor patients treated with scanned proton beams. Radiother Oncol 2020;144:127–34.
[43] Dutz A et al. Development and validation of NTCP models for acute side-effects resulting from proton beam therapy of brain tumours. Radiother Oncol 2019;130:164–71.
[44] Mankowski P et al. Optimizing radiotherapy for keloids: a meta-analysis systematic review comparing recurrence rates between different radiation modalities. Ann Plast Surg 2017;78:403–11.
[45] Fisher, Timing of surgery and radiotherapy in the management of metastatic spine disease: A systematic review. International Journal of Oncology, 2010. **36**
[46] ICRP, ICRP Statement on Tissue Reactions / Early and Late Effects of Radiation in Normal Tissues and Organs – Threshold Doses for Tissue Reactions in a Radiation Protection Context. ICRP, 2012. **41**
[47] P. Kumar, G.C.J., Modulation of wound healing in Swiss albino mice by different doses of gamma radiation Burns, 1995. **21**: p. 163-165
[48] Soliman H, Ruschin M, Angelov L, Brown PD, Chiang VLS, Kirkpat-rick JP, et al. Consensus contouring guidelines for postoperative completely resected cavity stereotactic radiosurgery for brain metas-tases. Int J Radiat Oncol Biol Phys 2018;100:436–42.
[49] Kim PH et al. Immune checkpoint inhibitor therapy may increase the incidence of treatment-related necrosis after stereotactic radiosurgery for brain metastases: a systematic review and meta-analysis. Eur Radiol 2021;31:4114–29.
[50] Minniti G et al. Current status and recent advances in resection cavity irradiation of brain metastases. Radiat Oncol 2021;16:73.